Optimal Power Allocation of GFDM Secondary Links With Power Amplifier Nonlinearity and ACI

Amirhossein Mohammadian, Mina Baghani, and Chintha Tellambura, *Fellow, IEEE*

***Abstract*—We investigate the problem of the rate maximization of a generalized frequency division multiplexing (GFDM) based secondary user (SU) link operating over a spectrum hole where adjacent channel interference (ACI) on two active primary users (PUs) in the right and left adjacent channels must be below a threshold. The SU transmitter has nonlinear power amplifier (PA) distortions. We consider a zero forcing (ZF) receiver which removes self-generated interference of GFDM. For a third-order nonlinear PA, we derive the signal-to-interference-plus noise ratio (SINR) and ACI. By using successive convex approximations, we develop a power allocation algorithm to maximize the SU rate subject to the ACI limits on adjacent PUs. Finally, we show that the proposed algorithm improves the SU data rate and that GFDM achieves a higher SU data rate than orthogonal frequency division multiplexing (OFDM).**

***Index Terms*—5G, GFDM, PA nonlinearity, cognitive radios.**

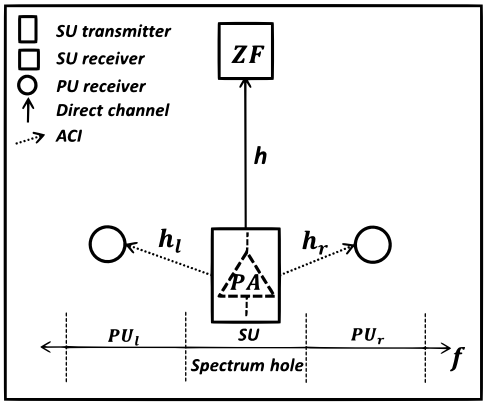

Fig. 1. The SU link and two active PU receivers in the right and left channels. GFDM transmission and ZF reception.

I. Introduction

DUE TO the forecasts of dramatic wireless traffic growth by 2020, spectrum scarcity is becoming a critical issue. One potential solution is the opportunistic access of spectrum holes (temporary unused spectrum bands of primary users (PUs)) by secondary (unlicensed) users (SUs). This opportunity is what motivates the concept of interweave cognitive radio (CR), where SUs sense and detect spectrum holes and access them. Thus in principle, if SU correctly detects a spectrum hole, its transmissions will not cause harmful interference on PUs [1].

However, 4G wireless radio uses traditional orthogonal frequency division multiplexing (OFDM), which exhibits relatively high levels of out-of-band (OOB) spectral leakages, causing strong interference into neighboring spectrum bands. Moreover, OOB increases due to non-ideal radio frequency (RF) hardware such as nonlinear power amplifiers (PAs). However, in densely packed spectrum bands, a spectrum hole is most likely to be surrounded by adjacent active PU bands. The OOB emissions of the SU utilizing this spectrum hole will then harm the PUs active on those bands. This is the main problem treated in this letter.

Manuscript received June 4, 2018; accepted July 9, 2018. Date of publication July 26, 2018; date of current version February 19, 2019. The associate editor coordinating the review of this paper and approving it for publication was P. Pawelczak. *(Corresponding author: Amirhossein Mohammadian.)*

A. Mohammadian and C. Tellambura are with the Department of Electrical and Computer Engineering, University of Alberta, Edmonton, AB T6G 2R3, Canada (e-mail: am11@ualberta.ca; chintha@ece.ualberta.ca).

M. Baghani is with the Electrical Engineering Department, Amirkabir University of Technology, Tehran 15875-4413, Iran (e-mail: baghani@aut.ac.ir).

Digital Object Identifier 10.1109/LWC.2018.2859921

An alternative to OFDM is generalized frequency division multiplexing (GFDM), which is a filtered multicarrier signal with low OOB emissions, high spectral efficiency and low latency [2]. Furthermore, cyclostationary detection performances of both GFDM and OFDM are similar [3], [4]. These advantages have made GFDM a potential contender for fifth generation (5G) wireless.

Thus, resource allocation has been investigated for GFDM based cognitive radio networks systems using metaheuristic methods [5], [6] and power allocations [7]. OOB emission due to non-linear PA has been studied [8]. However, the PA nonlinearity also causes in-band distortion, which should not be omitted. In [9] and [10], the power allocation for single carrier and multi-carriers cognitive radio is studied by considering nonlinear PA. To the best of our knowledge, power allocation for GFDM cognitive radios considering both OOB and in-band distortion has not been investigated before. This problem arises in the context of cognitive access to television white spaces.

In this letter, we consider the problem of an SU accessing a spectrum hole whose right and left neighboring channels consist two active PUs (Fig. 1). GFDM based, the SU transmitter includes a nonlinear PA. We consider a zero forcing (ZF) receiver which removes self-generated interference caused by non-orthogonality of GFDM subcarriers. We optimize the SU transmit power to maximize the SU link rate such that ACI on left and right PUs are below an acceptable interference threshold. The main contributions are as follows:

- The in-band distortion due to PA nonlinearity, signal-to-interference-plus noise ratio (SINR) and adjacent channel interference (ACI) are derived.

- The optimal power is allocated to the SU to maximize its rate subject to is both in-band distortion and OOB interference constraints. The optimization problem is non-convex, but we convert it to a standard geometric programming via the use of successive convex approximations.
- We solve this problem via the common CVX tool [11]. We compare both OFDM and GFDM and establish the benefits of a GFDM based interweave cognitive radios when the SUs suffer with a PA nonlinearity.

II. System Model

The SU (Fig. 1) transmits GFDM with *K* subcarriers carrying data of *M* time-slots. The GFDM modulator output per frame may be expressed as

$$y[n] = \sqrt{\alpha} \sum_{k=0}^{K-1} \sum_{m=0}^{M-1} x_{k,m} g_m[n] e^{j2\pi \frac{(k-\frac{K-1}{2})}{K} n} \tag{1}$$

where $x_{k,m}$ is independent and identically distributed (i.i.d.) data symbol with zero mean and unit variance on $k-th$ subcarrier of $m-th$ time-slot, $g_m[n] = g[n - mK]_{MK}$ is a circularly shifted version of normalized prototype filter $g[n]$ ($\sum_{n=0}^{MK-1} |g[n]|^2 = 1$) and α is average transmit power. The memoryless nonlinear PA has the polynomial function model:

$$z[n] = \sum_{i=0}^{2N_p+1} a_{2i+1} |y[n]|^{2i} y[n] \tag{2}$$

where a_{2i+1} are complex coefficients and the order of nonlinearity is $2N_p+1$. Since a third order polynomial is sufficient to model the PA accurately [10], we set $N_p = 1$. The Bussgang theorem [10] states that, for a Gaussian input, the output consists of a linear scaling of the input signal plus nonlinear distortion noise. But GFDM signal samples indeed become Gaussian as $MK \to \infty$ due to the central limit theorem [8].

After perfect synchronization, the receiver removes cyclic prefix and performs zero-forcing equalization in frequency domain. The received signal is thus $u[n] = z[n] + n_{eq}[n]$, where equivalent thermal noise component n_{eq} is the inverse fast Fourier transform of $\{\frac{N_t}{H}\}$, N_t and H are the thermal noise vector and the channel response in frequency domain, respectively. Finally, the estimated symbol at subcarrier k' and time slot m' is

$$\widehat{x}_{k',m'} = \sum_{n=0}^{MK-1} (u[n]) f^*_{m'}[n] e^{-j2\pi \frac{(k'-\frac{K-1}{2})}{K} n} \tag{3}$$

where $f_m[n] = f[n - mK]_{MK}$ is circularly shifted version of receive filter impulse response $f[n]$.

III. SINR Derivation

From (2) and (3), the detected symbol received at a given subcarrier and a time-slot can be expressed as

$$\widehat{x}_{k',m'} = \sqrt{\alpha} a_1 x_{k',m'} + n_{k',m'} + n_{eq,k',m'} \tag{4}$$

where $n_{eq,m',k'}$ is equivalent thermal noise in m' subsymbol of k' subcarrier and $n_{m',k'}$ is equivalent nonlinear distortion noise. The variance of the nonlinear distortion noise considering the third order of nonlinearity can be expressed as $\sigma^2_{n_{k',m'}} = \alpha^3 \Delta_{k',m'}$, where $\Delta_{k',m'}$ is equal to

$$\begin{aligned} \Delta_{k',m'} = |a_3|^2 K^3 \sum_{n=0}^{MK-1} \sum_{m_{1,2,3,4}=0}^{M-1} & f^*_{m'}[n] f_{(m'+m_3)_M}[n] \\ & g_{m_1}[n] g^*_{(m_1+m_3)_M}[n] g^*_{m_4}[n] g^*_{(m_2+m_3)_M}[n] \\ & (4 g_{m_4}[n] g_{(m_2+m_3)_M}[n] + 2 g_{m_2}[n] g_{(m_3+m_4)_M}[n]) \end{aligned} \tag{5}$$

where x_M denotes is x modulo M. Equation (5) is derived based on i.i.d. data symbols. Moreover, for reducing the computational complexity, we utilize the equality of $\sum_{k=0}^{K-1} e^{-j2\pi \frac{(k'-k)(n_1-n_2)}{K}} = K \sum_{t=0}^{M-1} \delta(n_1 - n_2 - tK)$. Due to space limitation, the proof of (5) is not presented. Finally, the SINR of estimated symbol of m' subsymbol of k' received subcarrier in SU receiver can be expressed as

$$\Gamma_{k',m'} = R_T \frac{\alpha |a_1|^2}{\sigma^2_{n_{k',m'}} + \sigma^2_{n_{eq,k',m'}}} = R_T \frac{\alpha |a_1|^2}{\alpha^3 \Delta_{k',m'} + \sigma^2_{n_{eq,k',m'}}} \tag{6}$$

where $R_T = \frac{MK}{MK+N_{CP}}$ and N_{CP} is the cyclic prefix length and $\sigma^2_{n_{eq,k',m'}}$ is given by [2]. Clearly, SINR (6) depends on α.

IV. ACI Derivation

To assess the ACI on the right and left PUs, we consider frequency selective channels which are constant over each subchannel which is accurate for small frequency bins. In order to derive ACI, we first need the power spectral density (PSD) of the GFDM output signal with a nonlinear PA. This has been derived for third order of nonlinearity as [8]

$$S_{ZZ}(f) = \alpha \eta_1(f) + \alpha^2 \eta_2(f) + \alpha^3 \eta_3(f) \tag{7}$$

where $\eta_1(f)$, $\eta_2(f)$ and $\eta_3(f)$ are expressed in (8), as shown at the bottom of the next page. Moreover, $G_m(f)$ is frequency response of each filter, T_s is one subsymbol duration and $\otimes$ denotes convolution. Therefore, the total ACI of SU on right channel could be derived as

$$P_r = \alpha T_{r,1} + \alpha^2 T_{r,2} + \alpha^3 T_{r,3} \tag{9}$$

where $T_{r,o} = \sum_{d=K+1}^{2K} H_r(d-K) \int_{f_d - 1/(2T_s)}^{f_d + 1/(2T_s)} \eta_o(f) df$, $o = 1, 2, 3$, $f_d = \frac{K+2d+1}{2T_s}$. Moreover, $H_r(d)$ is channel gain in $d-th$ frequency bin between SU transmitter in spectrum hole and PU receiver in right side. Similarly, the ACI related to the left channel can be derived. We omit the details for brevity.

V. Rate Maximization

The OOB (from nonlinear PA) on PUs must be lower than a specified interference threshold.Thus, according to (6) and (9), optimum SU power allocation can be formulated as

$$\begin{aligned} \max_{\alpha} \quad & \sum_{m'=0}^{M-1} \sum_{k'=0}^{K-1} \log(1 + R_T \frac{\alpha |a_1|^2}{\alpha^3 \Delta_{k',m'} + \sigma^2_{n_{eq,k',m'}}}) \\ s.t. \quad & \alpha T_{r,1} + \alpha^2 T_{r,2} + \alpha^3 T_{r,3} \le Q_r \\ & \alpha T_{l,1} + \alpha^2 T_{l,2} + \alpha^3 T_{l,3} \le Q_l \\ & \alpha \le P_{\max} \end{aligned} \tag{10}$$

where Q_r and Q_l are the maximum tolerable interference on the right and left PUs, respectively. The constraints force that the average transmit power should be lower than

$$\alpha < P'_{max} = \min\{P_{\max}, root^{+}(\alpha T_{r,1} + \alpha^2 T_{r,2} + \alpha^3 T_{r,3} - Q_r), root^{+}(\alpha T_{l,1} + \alpha^2 T_{l,2} + \alpha^3 T_{l,3} - Q_l)\} \quad (11)$$

where $root^{+}(f(x))$ stands for the set of the real positive roots of $f(x) = 0$. The problem can be converted minimization as

$$\min_{\alpha} \sum_{m'=0}^{M-1} \sum_{k'=0}^{K-1} -\log(1 + R_T \frac{\alpha |a_1|^2}{\alpha^3 \Delta_{k',m'} + \sigma^2_{n_{eq,k',m'}}}). \quad (12)$$

Due to the left and right interference constraints, this optimization problem is not convex. Thus, we use the successive convex approximation iteratively until convergence. First, the objective function is transformed to a logarithm of a multiplication of the terms:

$$\min_{\alpha} \log \prod_{m'=0}^{M-1} \prod_{k'=0}^{K-1} (1 + R_T \frac{\alpha |a_1|^2}{\alpha^3 \Delta_{k',m'} + \sigma^2_{n_{eq,k',m'}}})^{-1}. \quad (13)$$

The fractional term of SINR is converted to the posynomial function by arithmetic-geometric mean approximation [11]. This method converts the ratio $F(x) = \frac{\sum_{k=1}^{N_f} f_k(x)}{\sum_{i=1}^{N_g} g_i(x)}$ to the posynomial function as

$$\tilde{F}(x(t)) = \sum_{k=1}^{N_f} f_k(x) \left(\prod_{i=1}^{N_g} \left(\frac{g_i(x(t))}{\eta_i(t)} \right)^{\eta_i(t)} \right) \quad (14)$$

where $\eta_i(t) = \frac{g_i(t-1)}{\sum_{i'=1}^{N_g} g_{i'}(t-1)}$. Thus, our problem is converted to

$$\min_{\alpha(t)} \prod_{m'=0}^{M-1} \prod_{k'=0}^{K-1} (\alpha^3(t)\Delta_{k',m'} + \sigma^2_{n_{eq,k',m'}})(A(t-1))^{-\frac{\sigma^2_{n_{eq,k',m'}}}{A(t-1)}} \left(\frac{\alpha^3(t)\Delta_{k',m'}}{\frac{\alpha^3(t-1)\Delta_{k',m'}}{A(t-1)}}\right)^{-\frac{\alpha^3(t-1)\Delta_{k',m'}}{A(t-1)}} \left(\frac{R_T\alpha(t)|a_1|^2}{\frac{R_T\alpha(t-1)|a_1|^2}{A(t-1)}}\right)^{-\frac{R_T\alpha(t-1)|a_1|^2}{A(t-1)}} \quad (15)$$

where

$$A(t-1) = R_T\alpha(t-1)|a_1|^2 + \alpha^3(t-1)\Delta_{k',m'} + \sigma^2_{n_{eq,k',m'}} \quad (16)$$

Algorithm 1 Power Allocation Algorithm

1: Initialize the maximum number of iteration $I_{\max}$ and convergence condition ε.
2: Set $t \leftarrow 1$ and initialize $\alpha(0) = P'_{max}$ and Calculate $A(0)$ according to (16).
3: **do while** $|\alpha(t) - \alpha(t-1)| \leq \varepsilon$ and $t < I_{\max}$
4: Derive $\alpha(t)$ by solving GP optimization problem with objective function (15) and constraint $\alpha(t) < P'_{max}$.
5: Update A(t) by $\alpha(t)$ according to (16).
6: $t \leftarrow t + 1$
7: **end do**
8: **return**

and t is the iteration index. This (15) is a standard geometric program and can be solved by Algorithm 1 utilizing the CVX tool, which uses interior point method [11]. The number of iterations is $\frac{\log(c/t_0\beta)}{\log(\eta)}$, where c, t_0, $0< \beta <1$ and η are the number of constraint, initial point to approximate the accuracy of interior point method, the stopping criterion for interior point method and updating the accuracy of interior point method [11]. In our problem, the computation required for the arithmetic-geometric mean approximation in each iteration is $A = KM$. Thus, the total computational complexity is $A\frac{\log(1/t_0\beta)}{\log(\eta)}$.

Remarks:

1) Due to the use of GFDM and PA nonlinearity, allocation different powers for different subcarriers appears intractable. This problem is a future research topic.
2) We assume all channel state information (CSI) for the links is available for the SU transmitter [10].

VI. Numerical Results

The GFDM system consists of 64 subcarriers, 9 subsymbols and the raised-cosine prototype filter with roll-off-factor 0.3, and input data symbols are chosen from 16-QAM (quadrature amplitude modulation) with unit power. Moreover, sample time interval is normalized to one and number of channel taps (L) and N_{CP} are equal to 10. The channel power delay profile is exponential with the tap power $\sigma_i = 1/\sum_{k=0}^{L-1} e^{(i-k)/2},\ i = 0, \ldots, L-1$. We consider two non-linear devices: (1) PA_1 with the polynomial coefficients $a_1 = 15.0008 + j0.0908$ and $a_3 = -23.0826 + j3.3133$ [10]

$$\eta_1(f) = \frac{|a_1|^2}{M T_s} \sum_{k=0}^{K-1} \sum_{m=0}^{M-1} \left| G_m(f - \frac{(k - \frac{K-1}{2})}{T_s}) \right|^2$$

$$\eta_2(f) = 4real(a_1 a_3^*) \frac{K}{M T_s} \left(\sum_{m=0}^{M-1} \sum_{m'=0}^{M-1} (G_m(f) \otimes |G_{m'}(f)|^2) \times G_m^*(f) \right) \otimes \sum_{k=0}^{K-1} \delta(f - \frac{k - \frac{K-1}{2}}{T_s})$$

$$\eta_3(f) = \left(4|a_3|^2 \frac{K^2}{M T_s} \left(\sum_{m=0}^{M-1} \sum_{m'=0}^{M-1} \sum_{m''=0}^{M-1} (G_m(f) \otimes |G_{m'}(f)|^2 \otimes |G_{m''}(f)|^2) \times G_m^*(f) \right) \otimes \sum_{k=0}^{K-1} \delta(f - \frac{k - \frac{K-1}{2}}{T_s}) \right) + \left(\begin{array}{l} \frac{2|a_3|^2}{M T_s} \left(\sum_{m=0}^{M-1} \sum_{m'=0}^{M-1} \sum_{m''=0}^{M-1} (G_m(f) \otimes G_{m'}(f) \otimes G_{m''}^*(-f)) \times (G_m^*(f) \otimes G_{m'}^*(f) \otimes G_{m''}(-f)) \right) \\ \otimes \sum_{k=0}^{K-1} \sum_{k'=0}^{K-1} \sum_{k''=0}^{K-1} \delta(f - \frac{k + k' - k'' - \frac{K-1}{2}}{T_s}) \end{array} \right) \quad (8)$$

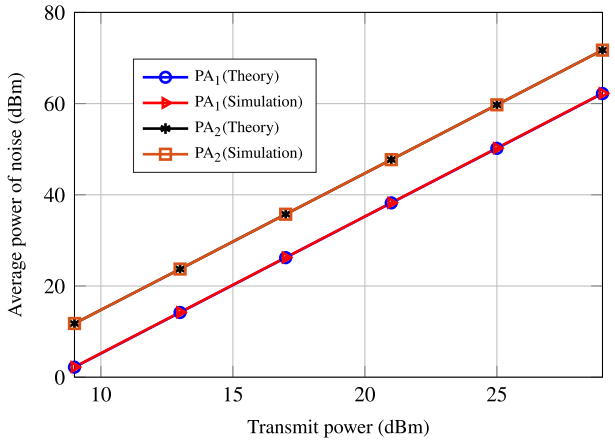

Fig. 2. Average noise power versus average transmit power α.

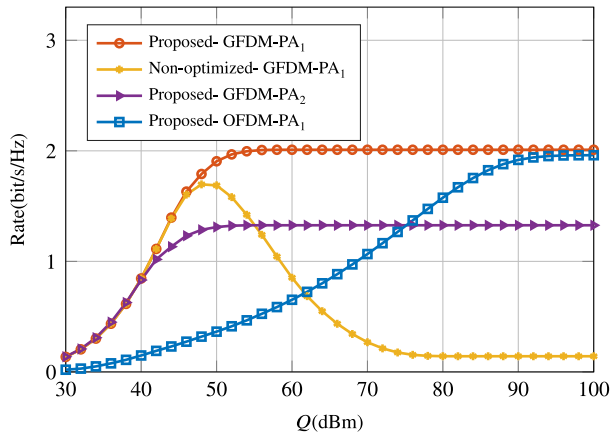

Fig. 3. Average rate of SU versus interference threshold limits.

and $P_{max} = \alpha_{sat} = 29$ dBm, that is derived from [8]; (2) PA_2 with $\{a_1, 3a_3\}$ and $P_{max} = \alpha_{sat} = 22$ dBm

The nonlinear distortion noise against transmit power is plotted in Fig. 2. Clearly, the simulation and theoretical results match perfectly and show the accuracy of derivation (5). Note that nonlinear noise increases with transmit power. This is because when the PA is driven close to the saturation point and the effect of the nonlinearity magnifies. Furthermore, since PA_2 has a more severe non-linearity, its nonlinear noise is more than that of the PA_1.

In Fig. 3, we set identical interference thresholds for right and left channels ($Q_r = Q_l = Q$) and plot the average SU rate achieved by the proposed algorithm. For comparison purposes, we also plot the rate of the non-optimized algorithm with maximum power limited per (11). Obviously, when Q is lower than 46 dBm, both algorithms achieve the same rate. But, when Q increases beyond 46 dBm, the proposed algorithm provides higher rate. This is because as Q increases, the non-optimized algorithm simply allocates more power according to (11), but then $P'_{\max}$ approaches the saturation point $P_{\max}$, which aggravates the nonlinear distortion noise and decreases the rate. However, the power allocated by the proposed algorithm is in the linear region of the PA. For this reason, the proposed algorithm mitigates the nonlinearity and achieves the best average rate. We also test the proposed algorithm with 64-subcarrier OFDM. That allows us to observe that GFDM outperforms OFDM under PA nonlinearity, which is due to lower OOB and higher spectral efficiency of GFDM.

Furthermore, in comparing PA_1 and PA_2, Fig. 3 shows that the latter achieves a lower rate. The reason is that since PA_2 has increased nonlinear distortion noise (Fig. 2), the SU rate with PA_2 decreases significantly. Thus, the detrimental effects of PA nonlinearity directly manifests on a system level.

VII. Conclusion

In this letter, we investigated an agile GFDM SU node which operates over a spectrum hole located in densely packed PU bands. In this scenario, the OOB emissions due to the non-linear PA of the SU will impact the adjacent PUs. We have derived the SINR and ACI and formulated the power allocation problem. The power is allocated to maximize the SU rate while minimizing both in-band distortion and OOB interference. Although this problem is non-convex, we converted it to a standard geometric programming problem via the use of successive convex approximations. Simulations show the accuracy of derived theoretical results and the benefits of the proposed power allocation. Finally, we find the use of GFDM rather than OFDM improves the SU rate in the presence of a PA nonlinearity.

References

[1] S. Atapattu, C. Tellambura, and H. Jiang, *Energy Detection for Spectrum Sensing in Cognitive Radio*. New York, NY, USA: Springer, 2014.

[2] N. Michailow *et al.*, "Generalized frequency division multiplexing for 5th generation cellular networks," *IEEE Trans. Commun.*, vol. 62, no. 9, pp. 3045–3061, Sep. 2014.

[3] R. Datta, N. Michailow, S. Krone, M. Lentmaier, and G. Fettweis, "Generalized frequency division multiplexing in cognitive radio," in *Proc. 20th Eur. Signal Process. Conf.*, Bucharest, Romania, 2012, pp. 2679–2683.

[4] D. Panaitopol, R. Datta, and G. Fettweis, "Cyclostationary detection of cognitive radio systems using GFDM modulation," in *Proc. IEEE Wireless Commun. Netw. Conf. (WCNC)*, Shanghai, China, 2012, pp. 930–934.

[5] A. A. Rosas, M. Shokair, and S. A. El-Dolil, "Proposed optimization technique for maximization of throughput under using different multicarrier systems in cognitive radio networks," in *Proc. 2nd Int. Conf. Electron. Eng. Clean Energy Green Comput. (EEECEGC)*, 2015, pp. 25–33.

[6] A. E. M. Dawoud, A. A. Rosas, M. Shokair, M. Elkordy, and S. El Halafawy, "PSO-adaptive power allocation for multiuser GFDM-based cognitive radio networks," in *Proc. Int. Conf. Sel. Topics Mobile Wireless Netw. (MoWNeT)*, 2016, pp. 1–8.

[7] A. Mohammadian, M. Baghani, and C. Tellambura, "Analysis and rate optimization of GFDM? Based cognitive radios," *Trans. Emerg. Telecommun. Technol.*, Jun. 2018, Art. no. e3435, doi: 10.1002/ett.3435.

[8] A. Mohammadian, A. Mohammadi, A. Abdipour, and M. Baghani, "Spectral analysis of GFDM modulated signal under nonlinear behavior of power amplifier," *eprint arXiv:1803.02026*, Mar. 2018. [Online]. Available: https://arxiv.org/abs/1803.02026

[9] M. Majidi, A. Mohammadi, and A. Abdipour, "Analysis of the power amplifier nonlinearity on the power allocation in cognitive radio networks," *IEEE Trans. Commun.*, vol. 62, no. 2, pp. 467–477, Feb. 2014.

[10] M. Baghani, A. Mohammadi, M. Majidi, and M. Valkama, "Analysis and rate optimization of OFDM-based cognitive radio networks under power amplifier nonlinearity," *IEEE Trans. Commun.*, vol. 62, no. 10, pp. 3410–3419, Oct. 2014.

[11] S. Parsaeefard, R. Dawadi, M. Derakhshani, and T. Le-Ngoc, "Joint user-association and resource-allocation in virtualized wireless networks," *IEEE Access*, vol. 4, pp. 2738–2750, 2016.